

Widely Emission-Tunable Alloyed ZnSeTe Quantum Dots: Blue-to-Red Emitters

Heesun Yang*, Sun-Hyoung Lee, Dae-Yeon Jo, Suk-Young Yoon, Hyun-Min Kim, Yuri Kim, Yang-Hee Kim, Seong Min Park

hyang@hongik.ac.kr

Department of Materials Science and Engineering, Hongik University, Seoul, 04066 Korea

Keywords: ZnSeTe, Non-Cd, Quantum Dots, Visible Emitters

ABSTRACT

Beyond InP quantum dots (QDs) ternary ZnSeTe QDs are emerging as non-Cd visible emitters. Their emissivity is widely tunable from blue to red simply by composition-controlled band gap engineering. We present highly efficient blue, green and red ZnSeTe QDs with relevant core/shell heterostructures and their potentials for QD display devices.

1 Introduction

Outstanding features of semiconductor quantum dots (QDs) including wide emission tunability, high photoluminescence quantum yield (PL QY), and narrow emissivity make them highly demanded especially for next-generation display and lighting devices [1–3]. Owing to the recent progress in synthesis along with core/shell heterostructural design, emissive performances of some III-V and I-III-VI-based environmentally benign QDs have rapidly approached those of Cd-based counterparts [4–6]. Among them, InP QDs have attracted great attention due to their exceptionally bright, narrow emissivity.

Synthesis of ternary ZnSeTe QDs have been initiated as potential blue emitters alternative to InP ones. Since the pioneering work on synthesis of blue-emissive ZnSeTe QDs and their application to the fabrication of blue QD-light-emitting diodes (QLEDs) or electroluminescent (EL) devices [7], there has been a rapid progress in synthetic methodologies of ZnSeTe QDs. Omata's group modulated the chemical composition toward Te-richer ZnSeTe to demonstrate green emissivity [8]. Although such Te-rich ZnSeTe QDs yielded highly poor PL QY along with a distinct defect emission, yet it opened a gateway for further improvements. In this contribution, we introduce Se/Te ratio-varied synthesis of highly fluorescent blue-, green-, red-emissive ZnSeTe QDs with their own core/shell heterostructures along with particular highlights on the applications to EL devices and color conversion LEDs from blue and green QD emitters, respectively.

2 Experiment

Overall synthesis of blue, green, and red ZnSeTe cores was by and large similar, mainly following our earlier protocols reported in literatures [9,10], while only changing Se/Te molar ratio for individual colored cores. After growth of core, double shellings of ZnSe/ZnS were adopted for blue QDs while triple shellings of ZnSe/ZnSeS/ZnS were implemented for both green and red QDs.

Multilayered QLEDs, consisting of ITO/poly(ethylenedioxythiophene):polystyrenesulfonate (PEDOT:PSS)/poly[(9,9-dioctylfluorenyl-2,7-diyl)-co-(4,4'-(N-(4-sec-butylphenyl)diphenylamine))] (TFB) hole

transport layer (HTL)/QD emitting layer (EML)/ZnMgO nanoparticles (NPs) electron transport layer (ETL)/Al, were fabricated via sequentially spin-casting all functional layers.

3 Results and Discussion

First, blue-emissive ZnSeTe core/shell QDs with dual shells of ZnSe/ZnS were synthesized. To examine the effects of core size and ZnSe shell thickness on PL and EL performances, small and large ZnSeTe cores with the respective diameters of 3.7 and 5.4 nm were prepared and then two different ZnSe thicknesses (i.e., thin-ZnSe and thick-ZnSe) were individually generated on such small and large cores (Fig. 1a-d). As shown in PL spectra of the resulting four core/shell QDs (Fig. 1e), large cores exhibited red-shifted PL relative to small ones as a result of quantum size effects and thick-ZnSe shell gave rise to more red-shifts in given core size due to a more electron delocalization to ZnSe shell. Overall PL QYs were rather higher from small core samples (70-73%) relative to large ones (52-53%) due to the surface area (or size) effects [11]. A series of blue ZnSeTe core/shell QDs were then employed as EML for QLED fabrication (Fig. 1f). As presented in Fig. 1g of the variation of external quantum efficiency (EQE) versus luminance of such heterostructurally different ZnSeTe QDs, large-core/thick-ZnSe/ZnS QDs gave the highest EQE of 11.4% and small-core/thin-ZnSe/ZnS QDs yielded the lower one of 8.4%, while EQEs from other two QDs were similar and intermediate (9.9-10.0%). Superior EQE from large-core/thick-ZnSe/ZnS QDs can result mainly from

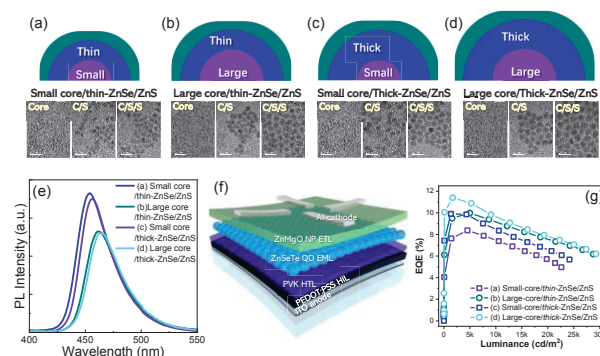


Fig. 1 Heterostructural schematics and TEM images of blue-emissive (a) small-core/thin-ZnSe/ZnS, (b) large-core/thin-ZnSe/ZnS, (c) small-core/thick-ZnSe/ZnS, and (d) large-core/thick-ZnSe/ZnS QDs and their (e) PL spectra, (f) QLED device structure, and (g) variation of EQE versus luminance.

the effective mitigation of Auger recombination synergically benefiting from larger core volume (from large core size) and more extensive electron wavefunction into ZnSe shell (from thick ZnSe).

Then, while fixing the feeding ratio of Se/Te of 4, a set of different-sized green-emissive ZnSeTe cores were prepared by controlling reaction temperature and injecting additional growth precursors. For convenience's sake, four sizes of small, medium, large, and the largest cores are referred to as core 1, 2, 3, and 4, respectively. As shown in Fig. 2a, the size evolution from 3.1 nm for core 1 up to 7.0 nm for core 4 can be verified. Systematic red-shift in PL with increasing core size result purely from quantum confinement effects (Fig. 2b). Size-dependent molar absorption coefficient (ϵ) values of ZnSeTe cores were derived using the Beer-Lambert law and the resulting molar absorption coefficient spectra as a function of wavelength for different-sized ZnSeTe cores are shown in Fig. 2c, exhibiting systematic, notable increase in molar absorption coefficient with larger ZnSeTe core size. Size-dependent ϵ values of a series of ZnSeTe cores along with green-emissive InP core at 450 nm were compared in Fig. 2d. The $\epsilon_{450 \text{ nm}}$ of ZnSeTe cores with size variation can be fitted to the relation of $\epsilon = 1011d^{3.12}$, nearly scaling with the core volume. These different-sized ZnSeTe cores were subjected identically to triple shellings of ZnSe/ZnSeS/ZnS. Fig. 3e displays normalized PL spectra of identically triple-shelled QDs of four different-sized cores, ranging from 509 nm for core 1 to 530 nm for core 4 in peak wavelength. PL QY tended to gradually decrease from 92% for core 1 down to 80% for core 4 again owing to surface area effects.

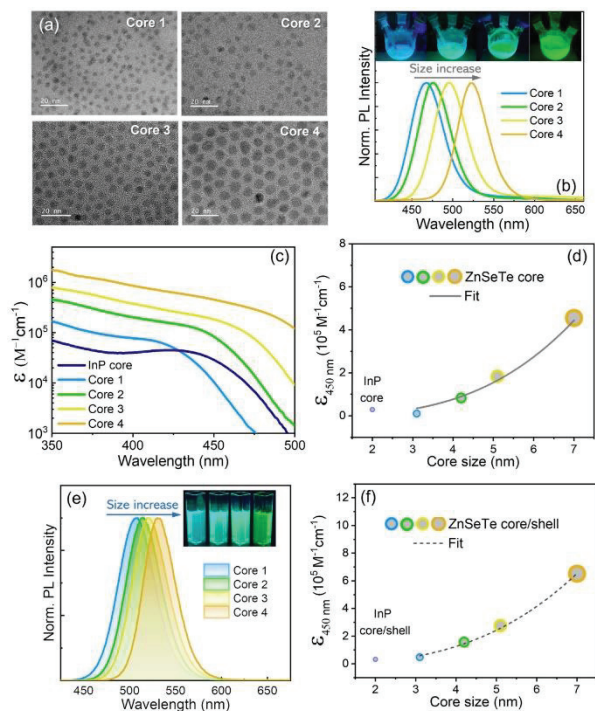


Fig. 2 (a) TEM images, (b) normalized PL spectra, (c) molar absorption coefficient spectra, and (d) $\epsilon_{450 \text{ nm}}$ of four different-sized green-emissive ZnSeTe cores. (e) Normalized PL spectra and (f) $\epsilon_{450 \text{ nm}}$ of a series of ZnSeTe/ZnSe/ZnSeS/ZnS core/shell QDs.

The ϵ values of a series of ZnSeTe/ZnSe/ZnSeS/ZnS and InP/ZnSe/ZnS QDs recorded at 450 nm were shown in Fig. 2f. Analogous to the ϵ - d result from ZnSeTe cores (Fig. 2d), $\epsilon_{450 \text{ nm}}$ of their core/shell QDs also scales with volume, specially showing the relation of $\epsilon = 2120d^{2.95}$.

The Se/Te ratio was further extensively varied in synthesis of ZnSeTe core. Absorption spectra of a set of such synthesized ZnSeTe cores and corresponding band gaps were plotted (Fig. 3a,b), well following the composition-dependent band gap bowing behavior of bulk $\text{ZnSe}_x\text{Te}_{1-x}$. Among the above ZnSeTe cores, ones synthesized with Se/Te ratios of 2 and 8 were chosen for triple shellings with ZnSe/ZnSeS/ZnS to demonstrate red emissivity. The former yielded a peak wavelength of 603 nm and PL QY of 56%, while the latter produced much longer emission wavelength of 668 nm but a negligible PL QY (i.e., <5%) (Fig. 3c). This indicates that excessively Te-richer ZnSeTe core will give rise to the substantial lattice mismatch between ZnSeTe core and ZnSe inner shell given a large disparity in ionic radius between Se^{2-} and Te^{2-} . For an effort to mitigate the possible interfacial strain, Se/Te=2-based ZnSeTe core was consecutively placed in additional core growth by controlling Se/Te feeding ratio. Upon applying an optimal Se/Te feeding ratio of 3 and after identical triple shellings, the resulting QDs displayed more red-shifted PL (608 nm) and enhanced PL QY (63%) (Fig. 3d,e), attributable to a further electron delocalization and reduced interfacial strain enabled by the additional ZnSeTe interlayer between ZnSeTe core and ZnSe inner shell.

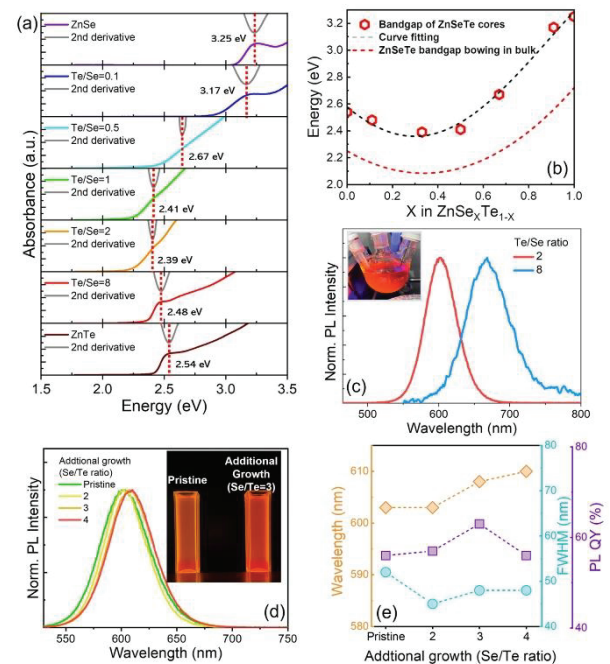


Fig. 3 (a) Original and the second derivative absorption spectra and (b) corresponding band gaps of ZnSeTe cores with a wide range of Te/Se ratios. (c) Normalized PL spectra of red-emissive ZnSeTe/ZnSe/ZnSeS/ZnS QDs with Se/Te ratios of 2 and 8 for core synthesis. (d) Normalized PL spectra of core/shell QDs produced by additional interfacial ZnSeTe layer with varied Se/Te ratios and (e) corresponding PL performances.

4 Summary

In this contribution, synthesis and optical properties of a set of ternary ZnSeTe QDs were introduced as environmentally benign full-color emitters of blue, green, and red color. In the case of blue QDs, the effects of core size and ZnSe shell thickness were explored in terms of PL and EL, particularly highlighting that large size of core was beneficial in acquiring EQE of EL device. Then, synthesis of four different-sized green-emissive ZnSeTe cores was then demonstrated and size-dependent molar absorption and PL characteristics of core and core/shell QDs were assessed. Lastly, to realize red emissivity from ZnSeTe composition, Se/Te ratio was extensively varied in core synthesis. The placement of appropriate additional ZnSeTe interlayer between highly Te-rich ZnSeTe core and ZnSe inner shell, where a substantial interfacial strain exists, was found to be effective in enhancing PL QY of red-emissive ZnSeTe QDs.

References

- [1] A. P. Litvin, I. V. Martynenko, F. Purcell-Milton, A. V. Baranov, A. V. Fedorov, Y. K. Gun'ko, *J. Mater. Chem. A* 5, 13252 (2017).
- [2] A. P. Alivisatos, *Science* 271, 933 (1996).
- [3] Y. Shirasaki, G. J. Supran, M. G. Bawendi, V. Bulovic, *Nat. Photonics* 7, 13 (2013).
- [4] Y. Kim, S. Ham, H. Jang, J. H. Min, H. Chung, J. Lee, D. Kim, E. Jang, *ACS Appl. Nano Mater.* 2, 1496 (2019).
- [5] H. Moon, W. Lee, J. Kim, D. Lee, S. Cha, S. Shin, H. Chae, *Chem. Commun.* 55, 13299 (2019).
- [6] Y. Li, X. Hou, X. Dai, Z. Yao, L. Lv, Y. Jin, X. Peng, *J. Am. Chem. Soc.* 141, 6448 (2019).
- [7] E.-P. Jang, C.-Y. Han, S.-W. Lim, J.-H. Jo, D.-Y. Jo, S.-H. Lee, S.-Y. Yoon, H. Yang, *ACS Appl. Mater. Interfaces* 11, 46062 (2019).
- [8] H. Asano, S. Tsukuda, M. Kita, S. Fujimoto, T. Omata, *ACS Omega* 3, 6703 (2018).
- [9] S.-H. Lee, C.-Y. Han, S.-W. Song, D.-Y. Jo, J.-H. Jo, S.-Y. Yoon, H.-M. Kim, S. Hong, J. Y. Hwang, H. Yang, *Chem. Mater.* 32, 5768 (2020).
- [10] C.-Y. Han, S.-H. Lee, S.-W. Song, S.-Y. Yoon, J.-H. Jo, D.-Y. Jo, H.-M. Kim, B.-J. Lee, H.-S. Kim, H. Yang, *ACS Energy Lett.* 5, 1568 (2020).
- [11] K. Gong, D. F. Kelly, *J. Phys. Chem. Lett.* 6, 1559 (2015).